The molecular beam epitaxial growth of GaAs/GaAs(111)B: doping and growth temperature studies

D. A. Woolf, Z. Sobiesierski, D. I. Westwood, and R. H. Williams

Citation: J. Appl. Phys. **71**, 4908 (1992); doi: 10.1063/1.350638
View online: http://dx.doi.org/10.1063/1.350638
View Table of Contents: http://jap.aip.org/resource/1/JAPIAU/v71/i10
Published by the American Institute of Physics.

Related Articles

CdSe/CdTe type-II superlattices grown on GaSb (001) substrates by molecular beam epitaxy
Appl. Phys. Lett. 100, 121908 (2012)

Effects of molecular beam epitaxy growth conditions on composition and optical properties of InxGa1−xBiyAs1−y
Appl. Phys. Lett. 100, 112110 (2012)

Investigation on the antiferromagnetic component in the intrinsic exchange bias in structurally single phase Cr2Te3 thin film
J. Appl. Phys. 111, 07D719 (2012)

Magnetism and transport properties of epitaxial Fe–Ga thin films on GaAs(001)
J. Appl. Phys. 111, 07C517 (2012)

The influence of Mg doping on the nucleation of self-induced GaN nanowires
AIP Advances 2, 012157 (2012)

Additional information on J. Appl. Phys.

Journal Homepage: http://jap.aip.org/
Journal Information: http://jap.aip.org/about/about_the_journal
Top downloads: http://jap.aip.org/features/most_downloaded
Information for Authors: http://jap.aip.org/authors

ADVERTISEMENT

Downloaded 02 Apr 2012 to 131.251.133.27. Redistribution subject to AIP license or copyright; see http://jap.aip.org/about/rights_and_permissions

The molecular beam epitaxial growth of GaAs/GaAs(111)B: doping and growth temperature studies

D. A. Woolf, Z. Sobiesierski, D. I. Westwood, and R. H. Williams
The Viriamu Jones Laboratory, Department of Physics and Astronomy, University of Wales College of Cardiff, P.O. Box 913, Cardiff, CF1 3TH, Wales, United Kingdom

(Received 9 December 1991; accepted for publication 31 January 1992)

A series of investigations are presented which address various aspects of the growth, by molecular beam epitaxy, of *n*-type (Si doped) *on-axis* GaAs/GaAs(111)B. *In situ* characterization by reflection high-energy electron diffraction has identified four surface phases on the static (zero growth rate) surface, and three reconstructions which occur, depending upon the substrate temperature, during growth. The *n*-type doping properties of GaAs/GaAs(111)B epilayers have been compared with *n*-GaAs/GaAs(100) structures. Hall effect and low-temperature photoluminescence measurements have demonstrated that it is possible to dope GaAs/GaAs(111)B with Si in the 6×10^{14} to 10^{18} cm^{-3} range. A variable growth temperature study is also presented which examines the surface structural, electrical, optical, and surface morphological properties of *n*-GaAs/GaAs(111)B grown in the 400 to 650 °C temperature range. The onset of electrical conduction, and optically active material, was found to be directly related to changes in the dynamic surface structure. The variable growth temperature study also revealed a temperature regime within which it was possible to significantly improve the surface morphology of on-axis GaAs/GaAs(111)B structures whilst retaining good electrical and optical properties.

I. INTRODUCTION

Several experiments concerning the growth of GaAs/GaAs(111)B are described within this paper. To prevent confusion regarding the designation of the substrate orientation, the following conventional protocol (Fig. 1) has been employed throughout this article: GaAs(111)A [or GaAs(111)] specifies the orientation where the surface As and Ga atoms are bound, respectively, by one and three back-bond(s) to the bulk GaAs; and GaAs(111)B [or GaAs($\bar{1}\bar{1}\bar{1}$)] describes the converse case, where the surface to bulk back-bonding is formed by one bond for the Ga atoms and three bonds for the As species. Thus, if the (111)A plane is regarded as the obverse side of a (111) wafer, then the reverse side would be the (111)B plane. Also, the convention of classifying the family of *all* (111) planes (both A and B) as {111} is invoked for the purpose of this investigation.

Even though some of the early molecular beam epitaxy (MBE) experiments of Cho[1] were concerned with the growth of GaAs/GaAs(111)B, the majority of homo- and heteroepitaxial GaAs-based structures have been deposited on the (100) crystallographic plane. In recent years, however, there has been renewed interest in the growth of materials on non-(100) orientated substrates. For example, the large piezoelectric effects encountered in lattice mismatched systems, such as $In_{0.1}Ga_{0.9}As$/GaAs{111}, are expected to yield exciting results for optoelectronic devices fabricated from these materials.[2,3] Furthermore, the growth of $Al_xGa_{1-x}As$/GaAs structures within etched "V" grooves on (100) substrates, where the exposed "V" faces belong to a set of {111} planes, has re-emphasized the need for an understanding of the growth of both binary and ternary III-V compounds on {111} crystals.[4]

A number of papers have addressed various aspects of the growth of GaAs/GaAs{111}. Ballingall and Wood[5] investigated the characteristics of dopant incorporation on the low-index orientations of GaAs [i.e., (100); (110); and (111)B]. The fact that Si acts as an *n*-type dopant for GaAs/GaAs(111)B, and is a *p*-type impurity for GaAs/GaAs(111)A was demonstrated by Wang *et al.* during their study of the growth of $Al_xGa_{1-x}As$/GaAs heterostructures.[6] Improvements in the electrical and optical properties of $Al_xGa_{1-x}As$ and GaAs epilayers were observed if GaAs(111)B-2°[100] misorientated substrates were used.[7] The doping characteristics of *p*-type, Si doped, GaAs/GaAs(111)A have been considered by Kadoya *et al.*,[8] and Shigeta *et al.*[9] Other studies have been concerned with improving the surface morphology of GaAs/GaAs(111)B to eradicate the {111} pyramid-type excrescences often encountered during growth.[10,11] Several research groups have also investigated the growth of $In_xGa_{1-x}As$/GaAs(111)B and $Al_xGa_{1-x}As$/GaAs(111)B [e.g., Refs. 12 and 13].

Despite this varied corpus of experimental data relating to the growth of GaAs-based compounds on GaAs(111)B substrates, there is not a published systematic study investigating either the Si doping of GaAs/GaAs(111)B compared with GaAs/GaAs(100), or the growth temperature dependence of the electrical and optical properties of GaAs/GaAs(111)B. This paper attempts to rectify this situation by presenting a series of MBE growth studies. First, the various surface phases of GaAs(111)B were examined by reflection high-energy electron diffraction (RHEED). Then the *n*-type doping

 © 1992 American Institute of Physics

Downloaded 02 Apr 2012 to 131.251.133.27. Redistribution subject to AIP license or copyright; see http://jap.aip.org/about/rights_and_permissions

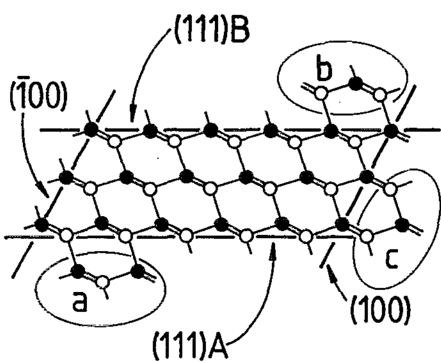

FIG. 1. The relationship between the (111)A, (111)B, and (100) crystallographic planes of a GaAs crystal. The open (○) and closed (●) circles represent, respectively, the Ga and As atoms. It is illustrated that for the (111)B plane each surface As atom has three back-bonds to the bulk crystal, whereas for each surface Ga atom only one such back-bond exists. The opposite case occurs on the (111)A surface. For the equivalent (100) and ($\bar{1}$00) planes the surface Ga and As atoms each have two substrate back-bonds. The insets (a), (b), and (c) show how Ga and As adatoms would bond to the "ideal" (i.e., unreconstructed) (111)A, (111)B, and (100) surfaces.

characteristics of GaAs/GaAs(111)B (using Si as the intentional impurity) were compared with similar *n*-type (Si doped) GaAs/GaAs(100) structures, grown over the doping range of $\simeq 4 \times 10^{14} \leqslant N \leqslant 10^{18}$ cm^{-3}. Finally, the variation of the electrical, optical, and surface morphological properties were compared for a standard 2 μm *n*-GaAs/GaAs(111)B structure, grown as a function of growth temperature (T_G) within the range $400 \leqslant T_G \leqslant 650$ °C. All of these studies were performed using *on-axis* GaAs(111)B substrates to demonstrate that, by optimizing the deposition conditions, it is possible to grow good electical and optical quality homoepitaxial GaAs(111)B without resorting to the use of misorientated substrates.

II. EXPERIMENTAL DETAILS

The growth experiments were performed in a VG Semicon V80H MBE reactor. Experimental details concerning the MBE flux calibrations have been presented elsewhere.[14] The MBE sample temperatures were obtained by calibrating the substrate heater thermocouple with an Ircon V Series optical pyrometer; this instrument has an operating temperature range of $450 \leqslant T \leqslant 1200$ °C. As a complementary method of substrate temperature calibration, the static (i.e., the zero growth rate) GaAs(100)-$c(4\times4)$ to (2×4) reversible surface phase was observed by RHEED. This $c(4\times4) \rightleftharpoons (2\times4)$ transition, which is only dependent upon the incident As_4 flux,[15] occurred at a temperature of $T_T = (525 \pm 5)$ °C, under the As_4 flux conditions employed for these experiments, i.e., $J_{As_4} \simeq 5\times10^{14}$ molecules cm^{-2} s^{-1}. This second method of temperature calibration proved to be particularly useful when the pyrometry measurements were invalidated by severe As coating of the pyrometer viewport.

Semi-insulating (Cr doped, $\rho \simeq 10^8$ Ω cm) *on-axis* GaAs(111)B substrate wafers, supplied by MCP Electronic Materials Ltd., were employed for these investigations. Each substrate was chemically etched in the following manner using choline-based Summa-clean and Summa-develop solutions, supplied by Mallinckrodt Inc. (Science Products Division). First, a 3 min ultrasonic degrease using Summa-clean was performed. After a 3 min deionized (DI) H_2O ($\rho \simeq 18\times10^6$ Ω cm) rinse, the sample was immersed in Summa-develop for $\simeq 12$ to 14 h. Following a 5 min DI H_2O rinse, the wafers were blow-dried with filtered N_2 gas, and then bonded with In solder onto standard VG Semicon solid Mo platters. The samples were then introduced, via a load-lock, into the MBE reactor. The desorption of the GaAs surface oxides was completed by (600 ± 10) °C when the substrate was annealed in the MBE reactor growth chamber, under the above quoted As_4 flux. The various stages of the MBE growth process were monitored *in situ* using a VG LEG110 15 kV RHEED system. After the thermal desorption of the surface oxide layer a strong bulk (1×1) RHEED pattern was observed together with a faint $(\sqrt{19}\times\sqrt{19})$ superlattice structure. The bulk features were intensity modulated along the length of the diffraction streaks. Such a pattern indicated that the oxide-free GaAs(111)B substrate surface was rough. However, by depositing 0.05 μm of GaAs at a rate of 1 μm/h, and at a temperature of 580 °C, it was possible to produce a smooth GaAs(111)B surface which displayed a sharp, prominent $(\sqrt{19}\times 19)$ surface reconstruction.

During the course of this study a variety of structures were grown investigating the *n*-type (Si) doping character and growth temperature dependence of GaAs/GaAs(111)B. The exact details of these structures (i.e., thickness and doping concentration) are presented later in this paper. Generally, all of the layers were grown at a rate of 1 μm/h, using an As_4 to Ga flux ratio of $J_{As_4}/J_{Ga} \simeq 0.8$, with the *n*-type doping concentration (N) and growth temperature (T_G) varied systematically within the ranges of mid-$10^{14} \leqslant N \leqslant 10^{18}$ cm^{-3} and $400 \leqslant T_G \leqslant 650$ °C, respectively.

After growth, each of the GaAs/GaAs(111)B structures was characterized *ex situ* by: Hall effect measurements at both room temperature and at 77 K (using a van der Pauw clover leaf sample with annealed In ohmic contacts), 4.2 and 10 K photoluminescence (PL), and Nomarski interference contrast microscopy.

III. RESULTS AND DISCUSSION

A. The surface phases of GaAs(111)B

Cho[1] reported the existence of the "As-rich" (2×2) and the "Ga-rich" $(\sqrt{19}\times\sqrt{19})R \pm 23.4°$ [hereafter referred to as $(\sqrt{19}\times\sqrt{19})$] surface reconstructions in the GaAs(111)B materials system; and yet GaAs(111)A only yielded a (2×2) surface phase.[16] The presence of the GaAs(111)B surface reconstructions was shown to be dependent upon the substrate temperature and/or the ratio of the incident As to Ga fluxes. The reversible transitions from the GaAs(111)B-(2×2) to the $(\sqrt{19}\times\sqrt{19})$ structures were shown to be analogous to the sundry surface phase transitions observed, under various growth conditions, in the GaAs(100) system.

Downloaded 02 Apr 2012 to 131.251.133.27. Redistribution subject to AIP license or copyright; see http://jap.aip.org/about/rights_and_permissions

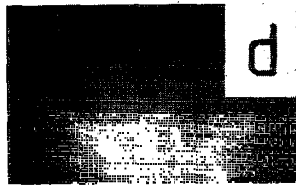

FIG. 2. A series of RHEED photographs, taken at various temperatures under an incident As_4 flux, of the four static GaAs(111)B surface phases: (a) (2×2), $T = 390$ °C; (b) $(1\times1)_{LT}$, $T = 545$ °C, (c) $(\sqrt{19}\times\sqrt{19})$, $T = 605$ °C; and, (d) $(1\times1)_{HT}$, $T = 645$ °C.

By mounting a GaAs(100) and GaAs(111)B sample side-by-side in the center of a Mo platter it was possible to employ the previously discussed GaAs(100)-$c(4\times4)$ $\rightleftharpoons(2\times4)$ transition [T_T = (525 ± 5) °C], under the quoted As_4 flux, as a fixed point for comparing and calibrating the GaAs(111)B surface phases. Following the removal of the GaAs surface oxides from both samples and the deposition of 0.05 μm of GaAs at T_G = 580 °C, sharp GaAs(100)-(2×4) and GaAs(111)B-$(\sqrt{19}\times\sqrt{19})$ RHEED patterns were obtained. By varying the substrate temperature the following, zero growth rate, reversible transitions (under the As_4 flux) between the GaAs(111)B surface phases were observed and measured: $(2\times2)\rightleftharpoons(1\times1)$ at T_{T1} = (545 ± 5) °C; $(1\times1)\rightleftharpoons(\sqrt{19}\times\sqrt{19})$ at T_{T2} = (555 ± 5) °C; and $(\sqrt{19}\times\sqrt{19})\rightleftharpoons(1\times1)$ at T_{T3} = (623 ± 5) °C. To distinguish between the two (1×1) surface phases, these will be labeled as $(1\times1)_{LT}$ and $(1\times1)_{HT}$, corresponding, respectively, to the low (LT) and high temperature (HT) phases. It may be, therefore, more appropriate to describe the $(\sqrt{19}\times\sqrt{19})$ surface phase as Ga-*stabilized*, and the $(1\times1)_{HT}$ structure as Ga-*rich*. Detailed soft x-ray photoelectron spectroscopy experiments are currently in progress to examine the stoichiometry of these various reconstructions. Figure 2 displays a series of photographs of RHEED patterns taken of the GaAs(111)B-(2×2), $(1\times1)_{LT}$, $(\sqrt{19}\times\sqrt{19})$, and $(1\times1)_{HT}$ reconstructions.

Chen *et al.*[17] also report the presence of an intermediate or "transition" surface phase, existing within a small temperature regime (≃30 °C), between the GaAs(111)B-(2×2) As-rich and $(\sqrt{19}\times\sqrt{19})$ "Ga-stabilized" reconstructions. This $(1\times1)_{LT}$ phase may be analogous to the GaAs(100)-(1×1) [sometimes described as (3×1)] state observed in the narrow temperature window (also ≃30 °C) between the As-stabilized (2×4) and Ga-stabilized (4×2) reconstructions.

To the best of our knowledge the GaAs(111)B-$(1\times1)_{HT}$ phase has not been previously reported, although Chen *et al.*[17] do provide specular beam RHEED data which decrease from a constant intensity for the $(\sqrt{19}\times\sqrt{19})$ phase to a less intense signal, corresponding to the existence of a very weak pattern with "five-fold fractional streaks," as the substrate temperature is increased to where we observe the $(1\times1)_{HT}$ state.

These four GaAs(111)B reversible phases were observed on all of the specimens prepared for these experiments. The $(1\times1)_{LT}\rightleftharpoons(\sqrt{19}\times\sqrt{19})$ surface phase transition temperature [T_{T2} = (555 ± 5) °C] was, therefore, adopted as the temperature reference point for the remainder of the GaAs(111)B growth studies.

B. *n*-GaAs/GaAs(111)B doping study

This study was initiated in order to compare the electrical and optical properties of *n*-type GaAs(111)B with *n*-GaAs(100), where Si was employed as the intentional impurity. After chemical etching, semi-insulating GaAs(111)B and GaAs(100) wafers were mounted side-by-side on each Mo sample holder. Following oxide desorption GaAs epilayers were grown at T_G = 580 °C, under the conditions described in Sec. II using Si dopant effusion cell temperatures (T_{Si}) in the range $800 \leqslant T_{Si} \leqslant 1040$ °C. The epilayer thickness (Θ) was adjusted to accommodate substrate-epilayer and epilayer-free surface depletion effects,[18] such that: for $T_{Si} = 800$ °C, $\Theta = 6$ μm; $T_{Si} = 900$ °C, $\Theta = 2$ μm; $T_{Si} = 960$ °C; $\Theta = 1$ μm; and, $T_{Si} = 1040$ °C, $\Theta = 1$ μm.

Figure 3 is a plot of the bulk Si doping concentration against Si dopant effusion cell temperature, determined from room temperature Hall effect measurements. For both orientations the epilayers were found to exhibit *n*-type conduction. Similar data were obtained from 77 K Hall effect measurements, indicating that on cooling the specimens to liquid nitrogen temperature very little, if any, carrier freeze-out occurred. The *n*-GaAs(100) samples followed the well-known N against T_{Si} trend encountered in previous studies.[19] The *n*-GaAs(111)B specimens showed a similar N against T_{Si} behavior, but in each case, with a slightly higher N value for a given T_{Si}. This difference in N between the two orientations, for a given Si dopant flux, could be attributed to the presence of a defect with donor-like properties within the GaAs/GaAs(111)B epilayers.

The fact that it was possible to grow *n*-type GaAs(111)B across the doping range from mid-10^{14} to 10^{18} cm^{-3} was most encouraging, especially since the earlier work of Ballingall *et al.*[5] produced highly resistive material compared with GaAs(100) grown at the same time which yielded $N \simeq 5\times10^{16}$ cm^{-3}. The investigations of Vina *et al.*[7] which also showed that on-axis GaAs(111)B

Downloaded 02 Apr 2012 to 131.251.133.27. Redistribution subject to AIP license or copyright; see http://jap.aip.org/about/rights_and_permissions

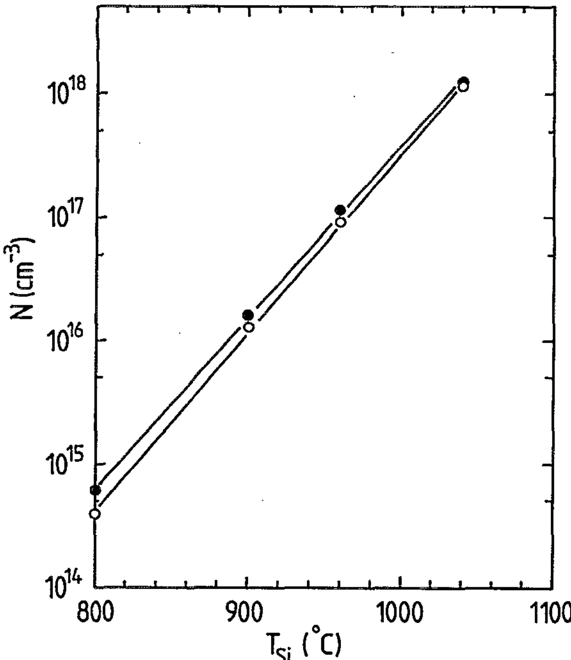

FIG. 3. Bulk Si doping as a function of Si dopant effusion cell temperature. Open symbols (○) correspond to GaAs/GaAs(100) epilayers, and the closed circles (●) relate to the GaAs/GaAs(111)B structures.

doped with Si at 10^{18} cm^{-3} was highly resistive. The possibility of unoptimized growth conditions on the non-(100) crystallographic planes, may be responsible for the differences between the electrical properties encountered in the previously reported studies, compared with this investigation.

Figure 4 displays the electron mobility ($\mu^{77\text{ K}}$) data for the n-GaAs(111)B and n-GaAs(100) samples, measured at liquid nitrogen temperature (77 K), plotted against N. The variation of $\mu^{77\text{ K}}$ with N for the GaAs(100) specimens followed the typical curves published for MBE-grown material compiled by Ilegems,[20] such that the samples doped at $N \simeq 6 \times 10^{14}$ cm^{-3} and 10^{18} cm^{-3} yielded $\mu^{77\text{ K}}$ values of 85 000 cm^2 V^{-1} s^{-1} and 2900 cm^2 V^{-1} s^{-1}, respectively. Except for the 10^{18}

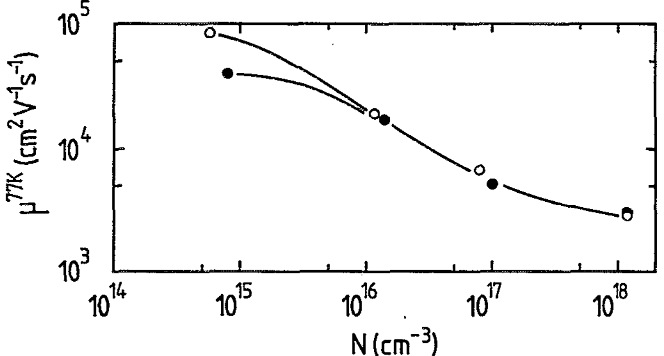

FIG. 4. 77 K electron mobility data as a function of n-type carrier concentration for the GaAs/GaAs(100) (○), and GaAs/GaAs(111)B (●) structures grown at a temperature of $T_G = 580$ °C.

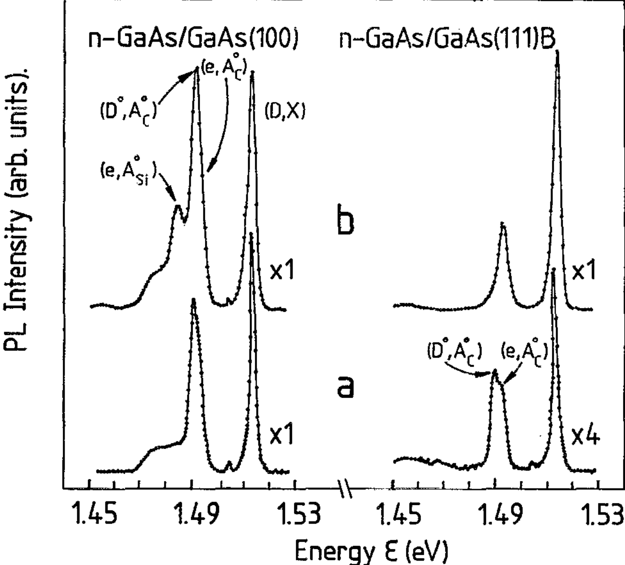

FIG. 5. 4.2 K photoluminescence spectra from homoepitaxial GaAs(100) and GaAs(111)B epilayers doped with Si such that: (a) $N \simeq 6 \times 10^{14}$ cm^{-3}, and, (b) $N \simeq 10^{16}$ cm^{-3}. The solid lines are only intended to provide a guide to the eye.

cm^{-3} sample where the n-GaAs(111)B and n-GaAs(100) $\mu^{77\text{ K}}$ values were about equal, the n-GaAs(100) 77 K electron mobilities were always higher than the n-GaAs(111)B case, despite the fact that both samples were doped with the *same* Si flux at the *same* time.

Figure 5 exhibits 4.2 K PL spectra obtained from n-GaAs(100) and n-GaAs(111)B samples, for bulk doping concentrations of $N \simeq 6 \times 10^{14}$ and $\simeq 10^{16}$ cm^{-3}. The GaAs(100) PL spectra exhibit the luminescence features usually observed for moderately doped n-type material. The excitonic PL, centered at $\epsilon = (1.5135 \pm 0.0005)$eV, contains unresolved components from both free and bound exciton emission. PL transitions at $\epsilon = 1.493$ eV (e,A^0_C) and at $\epsilon = 1.491$ eV (D^0,A^0_C) correspond to recombination involving carbon acceptors. Similarly, the PL peak energy of $\epsilon \simeq 1.485$ eV arises from recombination between electrons and Si acceptors (e,A^0_{Si}). The PL peak at $\epsilon \simeq 1.504$ eV, observed for the lower doped n-GaAs(100) layer, probably arises from point defects.[21] In comparison, the PL spectra for n-GaAs(111)B displayed essentially similar features, but with a distinctly different weighting between the separate donor–acceptor luminescence channels. For example, the intensity of the acceptor-related PL is significantly lower for the GaAs(111)B specimen than for the corresponding GaAs(100) sample doped with the same Si flux. In fact, there is no sign of any PL involving Si acceptors in either of the n-GaAs(111)B PL spectra displayed in Fig. 5. Photoluminescence measurements, performed on epilayers grown on misorientated GaAs(111)B substrates, have also suggested a lower carbon incorporation than that observed during the growth of GaAs/GaAs(100).[22] The observation of PL from the n-GaAs(111)B sample grown with the lowest doping level ($N \simeq 6 \times 10^{14}$ cm^{-3}) indicates a material quality far superior to anything previously

Downloaded 02 Apr 2012 to 131.251.133.27. Redistribution subject to AIP license or copyright; see http://jap.aip.org/about/rights_and_permissions

TABLE I. Surface reconstructions observed by RHEED during the homoepitaxial growth of GaAs(111)B.

Growth temp. T_G/°C	Surface reconstruction		
	Before growth	During growth	After growth
400	(2×2)	blurred spots	polycrystalline
500	(2×2)	$(1\times1)_{LT}$	(2×2)
520	(2×2)	$(1\times1)_{LT}$	(2×2)
545	$(1\times1)_{LT}$	$(1\times1)_{LT}/(\sqrt{19}\times\sqrt{19})$	(2×2)
550	$(1\times1)_{LT}/(\sqrt{19}\times\sqrt{19})$	$(1\times1)_{LT}/(\sqrt{19}\times\sqrt{19})$	$(1\times1)_{LT}$[a]
560	$(\sqrt{19}\times\sqrt{19})$	$(\sqrt{19}\times\sqrt{19})$	$(\sqrt{19}\times\sqrt{19})$[b]
570	$(\sqrt{19}\times\sqrt{19})$	$(\sqrt{19}\times\sqrt{19})$	$(\sqrt{19}\times\sqrt{19})$[b]
580	$(\sqrt{19}\times\sqrt{19})$	$(\sqrt{19}\times\sqrt{19})$	$(\sqrt{19}\times\sqrt{19})$[b]
600	$(\sqrt{19}\times\sqrt{19})$	$(\sqrt{19}\times\sqrt{19})$	$(\sqrt{19}\times\sqrt{19})$[b]
620	$(\sqrt{19}\times\sqrt{19})/(1\times1)_{HT}$	$(1\times1)_{HT}$	$(\sqrt{19}\times\sqrt{19})/(1\times1)_{HT}$[c]
635	$(1\times1)_{HT}$	$(1\times1)_{HT}$	$(1\times1)_{HT}$[d]
650	$(1\times1)_{HT}$	$(1\times1)_{HT}$	$(1\times1)_{HT}$[d]

Surface phase transitions observed on cooling in the As_4 flux after growth:

[a] $(1\times1)_{LT}\rightarrow(2\times2)$.

[b] $(\sqrt{19}\times\sqrt{19})\rightarrow(1\times1)_{LT}\rightarrow(2\times2)$.

[c] $(\sqrt{19}\times\sqrt{19})/(1\times1)_{HT}\rightarrow(\sqrt{19}\times\sqrt{19})\rightarrow(1\times1)_{LT}\rightarrow(2\times2)$.

[d] $(1\times1)_{HT}\rightarrow(\sqrt{19}\times\sqrt{19})\rightarrow(1\times1)_{LT}\rightarrow(2\times2)$.

reported in the literature for the growth of *on-axis* GaAs/GaAs(111)B.

C. *n*-GaAs/GaAs(111)B variable growth temperature study

A series of 2-μm-thick GaAs/GaAs(111)B structures was grown to investigate the electrical and optical properties of this materials system as a function of the growth temperature. All of the epilayers were grown with the fluxes and growth rate described in Sec. II, and with a constant Si dopant flux ($T_{Si}=900\,°C$, such that N was intended to be $\simeq10^{16}$ cm^{-3}). The growth temperature (T_G) for this series of samples was varied in a random fashion within the range $400\leqslant T_G\leqslant650\,°C$, as determined from the $(1\times1)_{LT}\rightleftharpoons(\sqrt{19}\times\sqrt{19})$ surface phase transition temperature. This growth temperature range encompasses the four surface phases observed on GaAs(111)B.

Table I details the surface reconstructions, as viewed by RHEED, before, during, and after the growth of the GaAs/GaAs(111)B samples. Whereas the four surface phases reported in Sec. III A were observed on the static surface under an As_4 flux (i.e., before and after growth), only the $(1\times1)_{LT}$, $(\sqrt{19}\times\sqrt{19})$, and $(1\times1)_{HT}$ surface structures were viewed during growth. It is interesting to note the absence of the (2×2) phase during growth. The sample grown at the lowest temperature ($T_G=400\,°C$) became polycrystalline during deposition, suggesting that for this materials system a structural order–disorder transition occurs between 400 and 500 °C. A similar order–disorder transition was encountered during the heteroepitaxial growth of GaAs(11$\bar{1}$)B/Si(111).[23] However, for the GaAs/GaAs(100) system this order–disorder transition is reported to occur between 70 and 90 °C.[24] These differences in behavior for the homoepitaxially grown GaAs(100) and GaAs(111)B imply that the growth mechanism is different for these two crystallographic orientations. Such differences between the growth of GaAs/GaAs(100) and GaAs/GaAs(111)B are not unexpected when it is considered (with reference to the insets in Fig. 1) that the incident Ga and As species are bound in different fashions on these two orientations. Consequently, the binding energies of the Ga and As adatoms, the acti-

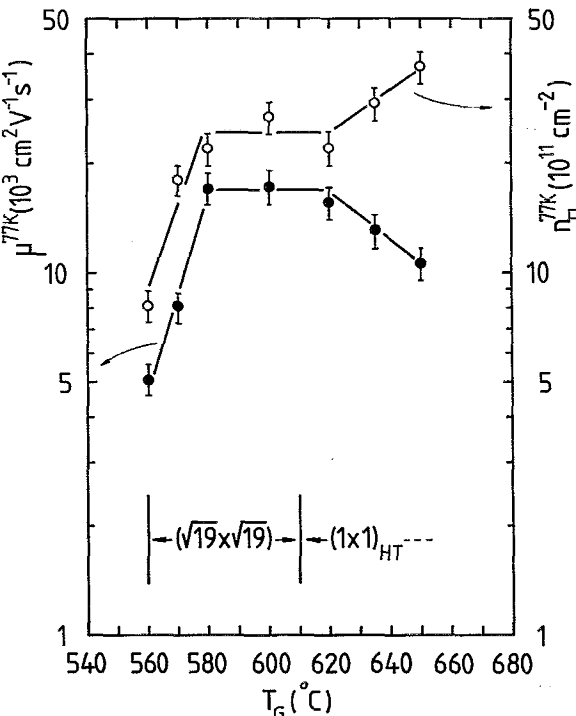

FIG. 6. 77 K electron mobility (●), and sheet carrier concentration (○) data as a function of growth temperature for a series of 2 μm *n*-GaAs/GaAs(111)B structures. The nominal sheet doping concentration for these samples was $n_{\square}\simeq2\times10^{12}$ cm^{-2}. Also indicated are the GaAs(111)B surface phases observed, by RHEED, *during* growth.

Downloaded 02 Apr 2012 to 131.251.133.27. Redistribution subject to AIP license or copyright; see http://jap.aip.org/about/rights_and_permissions

vation energies of the surface migration processes, and the migration paths of the surface species will be different for the GaAs(100) and GaAs(111)B crystallographic planes.

Data from the Hall effect measurements at liquid nitrogen temperature of the electron mobility ($\mu^{77\ K}$) and sheet carrier concentration ($n_{\square}^{77\ K}$), as a function of growth temperature, are illustrated in Fig. 6. Below $T_G = 560$ °C the GaAs(111)B samples were highly resistive. At, and above, $T_G = 560$ °C conduction was measurable; all of the epilayers exhibited n-type behavior. In the $560 \leqslant T_G \leqslant 580$ °C temperature range both $\mu^{77\ K}$ and $n_{\square}^{77\ K}$ increased to $\simeq 17\,000$ cm^2 V^{-1} s^{-1} and $\simeq 2.5\times10^{12}$ cm^{-2}, respectively. These values remained constant within the $580 \leqslant T_G \leqslant 620$ °C temperature regime; and then between $620 \leqslant T_G \leqslant 650$ °C, $\mu^{77\ K}$ steadily decreased to $\simeq 10\,000$ cm^2 V^{-1} s^{-1}, while $n_{\square}^{77\ K}$ increased to $\simeq 3.7\times10^{12}$ cm^{-2}. This reduction in $\mu^{77\ K}$ with the accompanying rise in $n_{\square}^{77\ K}$ may be simply due to the existence of electrically active defects with a donor-like behavior. Such defects could be associated with the fact that above 620 °C the GaAs growth was conducted under Ga-rich conditions, due to the depletion of As from the sample surface at these elevated temperatures.

The observed changes in electrical conduction can be directly related to the dynamic surface structure (i.e., surface reconstruction *during* growth) as determined by RHEED (Table I). When growing with a $(1\times1)_{LT}$ or mixed $(1\times1)_{LT}/(\sqrt{19}\times\sqrt{19})$ surface phase the resulting epilayer was highly resistive. The critical growth temperature (T_G^C) for the electrical conduction, and subsequent $\mu^{77\ K}$ and $n_{\square}^{77\ K}$ plateaux, corresponded to growth under the $(\sqrt{19}\times\sqrt{19})$ phase, whilst the $\mu^{77\ K}$ and $n_{\square}^{77\ K}$ turning points at the end of these plateaux were associated with the $(1\times1)_{HT}$ surface structure during growth. A similar critical temperature for the electrical conduction, related to a change in dynamic surface structure, has been reported for the n-GaAs/GaAs(100) system.[14,25] In the GaAs/GaAs(100) case it was found that the epilayers were highly resistive when growing with the As-*rich* $c(4\times4)$ or mixed $c(4\times4)/(2\times4)$ structures, and yet were conducting when deposited under As-*stabilized* (2×4) conditions. Miller *et al.*[26] have argued that the presence of point defects within the GaAs host crystal grown at low temperature (and thus under As-rich conditions), cause mid-band gap electronic states which compensate the intentional Si donors. Such a compensating mechanism, due to growth under As-rich conditions, may be responsible for the highly resistive GaAs(111)B material deposited below the $T_G \simeq 560$ °C critical temperature.

When comparing this n-GaAs/GaAs(111)B variable growth temperature study with the n-GaAs/GaAs(100) investigation conducted by Westwood *et al.*,[14] (under similar growth conditions and within the same MBE reactor), it is interesting to note that the critical temperature (T_G^C) for the electrical conduction occurs when changing from growth under As-rich to Ga-stabilized conditions for the (111)B case, instead of the alteration from growth under As-rich to As-stabilized conditions for the (100) system. A detailed surface science examination, comparing and contrasting the surface structure and chemistry, of the manifold GaAs(100) and GaAs(111)B reconstructions would provide a better understanding of the intrinsic differences between these two particular low-index crystallographic planes of GaAs.

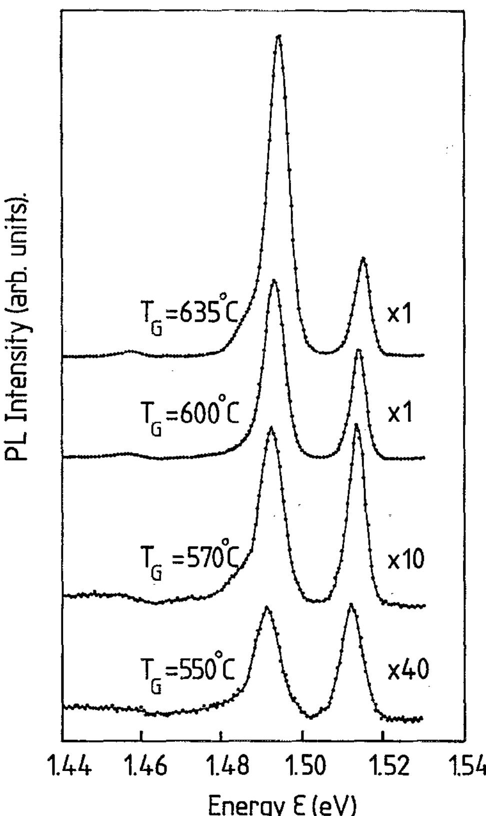

FIG. 7. 10 K photoluminescence spectra obtained from 2 μm n-GaAs/GaAs(111)B samples grown as a function of deposition temperature.

Figure 7 displays the evolution of the 10 K PL spectra, obtained from the n-GaAs(111)B layers, with growth temperature. No significant luminescence was observed for n-GaAs(111)B layers grown below 550 °C. For growth temperatures between 550 and 600 °C, the PL intensity increased dramatically with growth temperature. In fact, the integrated PL intensity continued to increase with growth temperature up to 635 °C, at which point it began to decrease slowly with further increases in temperature. Therefore, the PL and Hall effect data both suggest that the optical and electrical properties of n-GaAs(111)B significantly improve above a critical growth temperature ($550 \leqslant T_G^C \leqslant 560$ °C), corresponding to growth under Ga-stabilized conditions.

Nomarski interference contrast micrographs of a selection of the variable growth temperature samples are presented in Fig. 8. Pyramid-like surface features, as previously reported by Cho *et al.*,[16] were observed on these specimens. The size of these pyramids, and likewise the surface roughness of the samples, increased with growth temperature, reaching a maximum at $T_G \simeq 600$ °C. However, between $T_G = 600$ and 620 °C a transition occurred such that the surface became smoother, and the pyramid-like features were eliminated and replaced by widely

Downloaded 02 Apr 2012 to 131.251.133.27. Redistribution subject to AIP license or copyright; see http://jap.aip.org/about/rights_and_permissions

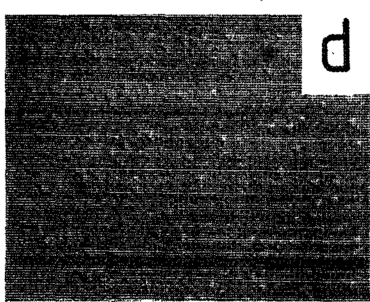

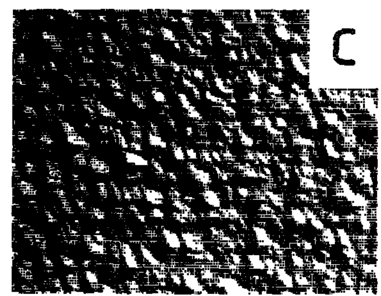

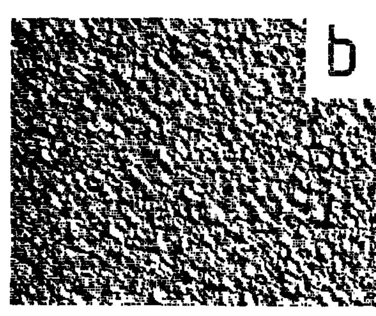

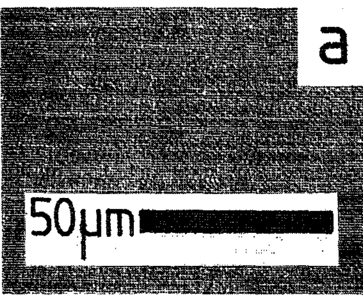

FIG. 8. Nomarski interference contrast micrographs of the surface morphologies of 2-μm-thick homoepitaxial GaAs(111)B structures grown at the following temperatures: (a) T_G = 400 °C; (b) T_G = 545 °C; (c) T_G = 580 °C; and, T_G = 620 °C. The scaling marker represents 50 μm.

spaced (typically $\simeq$10 μm) triangular defects. When viewed with the naked eye the samples with the pyramidal defects appeared "milky" or "frosty," whilst the asperity-free surfaces were shiny.

Chen *et al.*[17] report a growth temperature region of $\simeq$565 to 590 °C, within the ($\sqrt{19}\times\sqrt{19}$) plateau of their static GaAs(111)B surface phase map, in which pyramid-free growth occurred. The fact that our GaAs(111)B growth rate was approximately three times greater than that used by Chen *et al.*[17] (i.e., 1 μm/h compared with 0.3 μm/h) might account for the differences in the observed pyramid-free growth temperature windows. Effects due to discrepancies between our temperature calibrations and those of Chen *et al.* are unlikely, since in both cases the desorption of the GaAs(111)B surface oxides was determined to have been completed by within 10 °C of the same temperature, i.e., 590 °C (Refs. 10 and 17) compared with (600$\pm$10) °C (this study).

Takano *et al.*[11] achieve improvements in surface morphology, resulting in the growth of 1200-Å-thick mirror-like, pyramid-free GaAs(111)B epilayers by employing the migration enhanced epitaxy (MEE) technique. Whereas the success of the MEE process in producing such pyramid-free growth is not doubted, it remains unproven whether MEE can be repeatedly and reproducibly applied to the growth of thick ($\Theta > 1$ μm) structures.

To eliminate the possibility of unintentional substrate misorientation effects, a 2 μm GaAs/GaAs(111)B structure, doped with Si at $N\simeq 10^{16}$ cm^{-3}, was grown at T_G = 620 °C on an undoped on-axis GaAs(111)B wafer supplied by a different manufacturer (Sumitomo Electric Industries Ltd.). This test structure displayed a mirror-like, pyramid-free surface morphology, and yielded room temperature and 77 K Hall effect data equivalent to the sample grown at T_G = 620 °C on the MCP GaAs(111)B substrates.

In summary, the electrical, optical, and surface morphological observations imply that, for the growth conditions employed for these experiments, an optimum "growth temperature window" exists within the range $600 \leqslant T_G \leqslant 620$ °C for the deposition of *on-axis* *n*-GaAs/GaAs(111)B structures.

IV. CONCLUSIONS

MBE grown GaAs/GaAs(111)B surfaces have been characterized *in situ* by RHEED. Four static (zero growth rate) reversible surface phases have been identified, i.e., the As-rich (2$\times$2); the $(1\times1)_{LT}$ intermediate state; the Ga-stabilized ($\sqrt{19}\times\sqrt{19}$); and, the Ga-rich $(1\times1)_{HT}$. Only the $(1\times1)_{LT}$, ($\sqrt{19}\times\sqrt{19}$) and $(1\times1)_{HT}$ reconstructions were observed on the dynamic (growing) GaAs surface. A comparative doping study of the electrical and optical properties of homoepitaxial *n*-GaAs(111)B and *n*-GaAs(100) demonstrated that it is possible to dope GaAs(111)B epilayers with Si in the range $N\simeq$mid-10^{14} to 10^{18} cm^{-3}. During this study some evidence of increased conduction in *n*-GaAs/GaAs(111)B, due to the presence of a donor-like defect of uncertain origin, was apparent. The surface structural, electrical, optical, and surface morphological characteristics of 2 μm *n*-GaAs/GaAs(111)B structures were investigated as a function of growth temperature. It was possible to associate the on-set of *n*-type electrical conduction, together with significant improvements in the optical quality of the epilayers, to changes in the surface structure during growth. Furthermore, for the first time an optimum growth temperature window of 600 to 620 °C has been located for the deposition of smooth, conducting, optically active *on-axis* *n*-GaAs/GaAs(111)B structures.

Downloaded 02 Apr 2012 to 131.251.133.27. Redistribution subject to AIP license or copyright; see http://jap.aip.org/about/rights_and_permissions

ACKNOWLEDGMENTS

The authors wish to express their appreciation to Dr. C. C. Matthai (UWCC) for several useful and interesting discussions concerning the preparation of this paper. The Technical Staff of the Department of Physics and Astronomy (UWCC) are thanked for their assistance during these investigations. The financial support of the United Kingdom Science and Engineering Research Council (SERC) Low Dimensional Structures and Devices (LDSD) initiative is gratefully acknowledged.

[1] A. Y. Cho, J. Appl. Phys. **41**, 2780 (1970).
[2] D. L. Smith, Solid State Commun. **57**, 919 (1986).
[3] E. A. Caridi, T. Y. Chang, K. W. Goossen, and L. F. Eastman, Appl. Phys. Lett. **56**, 660 (1990).
[4] E. Kapon, J. P. Harbison, C. P. Yuin, and N. G. Stoffel, Appl. Phys. Lett. **52**, 607 (1988).
[5] J. M. Ballingall and C. E. C. Wood, Appl. Phys. Lett. **41**, 947 (1982).
[6] W. I. Wang, E. E. Mendez, T. S. Kuan, and L. Esaki, Appl. Phys. Lett. **47**, 826 (1985).
[7] L. Vina and W. I. Wang, Appl. Phys. Lett. **48**, 36 (1986).
[8] Y. Kadoya, A. Sato, H. Kano, and H. Sakaki, J. Cryst. Growth **111**, 280 (1991).
[9] M. Shigeta, Y. Okano, H. Seta, H. Katahama, S. Nishine, K. Kobayashi, and I. Fujimoto, J. Cryst. Growth **111**, 284 (1991).
[10] P. Chen, K. C. Rajkumar, and A. Madhukar, Appl. Phys. Lett. **58**, 1771 (1991).
[11] Y. Takano, M. Lopez, T. Torihata, T. Ikei, Y. Kanaya, K. Pak, and H. Yonezu, J. Cryst. Growth **111**, 216 (1991).
[12] K. Elcess, J.-L. Liévin, and C. G. Fonstad, J. Vac. Sci. Technol. B **6**, 638 (1988).
[13] S. M. Shank and G. W. Wicks, J. Cryst. Growth **111**, 440 (1991).
[14] D. I. Westwood, D. A. Woolf, and R. H. Williams, J. Cryst. Growth **98**, 782 (1989).
[15] J. H. Neave and B. A. Joyce, J. Cryst. Growth **44**, 387 (1978).
[16] A. Y. Cho, M. B. Panish, and I. Hayashi, *Proceedings 3rd International Symposium on GaAs and Related Compounds*, edited by K. Paulus (Institute of Physics, London, 1970), p. 18.
[17] P. Chen, K. C. Rajkumar and A. Madhukar, J. Vac. Sci. Technol. B **9**, 2312 (1991).
[18] A. Chandra, C. E. C. Wood, D. W. Woodard, and L. F. Eastman, Solid State Electron. **22**, 645 (1979).
[19] K. Ploog, *MBE of Artificially Layered Semiconductor Structures: Basic Concepts and Recent Achievements*, NATO ASI Series B, edited by P. Dhez and C. Weisbuch (Plenum, New York, 1988), Vol. 182.
[20] M. Ilegems, "Properties of III-V Layers," *The Technology and Physics of Molecular Beam Epitaxy*, edited by E. H. C. Parker (Plenum, New York, 1985).
[21] H. Künzel and K. Ploog, Appl. Phys. Lett. **37**, 416 (1980).
[22] A. Chin, P. Martin, P. Ho, J. Ballingall, T.-h. Yu, and J. Mazurowski, Appl. Phys. Lett. **59**, 1899 (1991).
[23] D. A. Woolf, D. I. Westwood, M. A. Anderson, and R. H. Williams, Appl. Surf. Sci. **50**, 445 (1991).
[24] J. H. Neave and B. A. Joyce, J. Cryst. Growth **43**, 204 (1978).
[25] S. M. Newstead, R. A. A. Kubiak, and E. H. C. Parker, J. Cryst. Growth **81**, 49 (1987).
[26] J. N. Miller and T. S. Low, J. Cryst. Growth **111**, 30 (1991).

Downloaded 02 Apr 2012 to 131.251.133.27. Redistribution subject to AIP license or copyright; see http://jap.aip.org/about/rights_and_permissions